PHYSICAL REVIEW D **85,** 034506 (2012)

Hyperon sigma terms for 2 + 1 quark flavors

R. Horsley,[1] Y. Nakamura,[2] H. Perlt,[3] D. Pleiter,[4,5] P. E. L. Rakow,[6] G. Schierholz,[5,7] A. Schiller,[3] H. Stüben,[8] F. Winter,[1] and J. M. Zanotti[1]

(QCDSF-UKQCD Collaboration)

[1]*School of Physics and Astronomy, University of Edinburgh, Edinburgh EH9 3JZ, United Kingdom*
[2]*RIKEN Advanced Institute for Computational Science, Kobe, Hyogo 650-0047, Japan*
[3]*Institut für Theoretische Physik, Universität Leipzig, 04109 Leipzig, Germany*
[4]*Jülich Supercomputing Centre, Forschungszentrum, Jülich, Germany*
[5]*Institut für Theoretische Physik, Universität Regensburg, 93040 Regensburg, Germany*
[6]*Theoretical Physics Division, Department of Mathematical Sciences, University of Liverpool, Liverpool L69 3BX, United Kingdom*
[7]*Deutsches Elektronen-Synchrotron DESY, 22603 Hamburg, Germany*
[8]*Konrad-Zuse-Zentrum für Informationstechnik Berlin, 14195 Berlin, Germany*

(Received 3 November 2011; published 22 February 2012)

QCD lattice simulations determine hadron masses as functions of the quark masses. From the gradients of these masses and using the Feynman-Hellmann theorem the hadron sigma terms can then be determined. We use here a novel approach of keeping the singlet quark mass constant in our simulations which upon using an $SU(3)$ flavor symmetry breaking expansion gives highly constrained (i.e. few parameter) fits for hadron masses in a multiplet. This is a highly advantageous procedure for determining the hadron mass gradient as it avoids the use of delicate chiral perturbation theory. We illustrate the procedure here by estimating the light and strange sigma terms for the baryon octet.

DOI: 10.1103/PhysRevD.85.034506 PACS numbers: 12.38.Gc

I. INTRODUCTION

Hadron sigma terms $\sigma_l^{(H)}$, $\sigma_s^{(H)}$ are defined[1] as that part of the mass of the hadron (for example the nucleon) coming from the vacuum connected expectation value of the up (u) down (d) and strange (s) quark mass terms in the QCD Hamiltonian,

$$\begin{aligned}\sigma_l^{(H)} &= m_l^R \langle H|(\bar{u}u + \bar{d}d)^R|H\rangle, \\ \sigma_s^{(H)} &= m_s^R \langle H|(\bar{s}s)^R|H\rangle,\end{aligned} \tag{1}$$

where we have taken the u and d quarks to be mass degenerate, $m_u = m_d \equiv m_l$. (The superscript R denotes a renormalized quantity.) Other contributions to the hadron mass come from the chromo-electric and chromo-magnetic gluon pieces and the kinetic energies of the quarks, [2]. Sigma terms are interesting because they are sensitive to chiral symmetry breaking effects. Experimentally the value for $\sigma_l^{(N)}$ has been deduced from low energy π-N scattering. A delicate extrapolation to the chiral limit [1] gives a result for the isospin even amplitude of $\sigma_{\pi N}/f_\pi^2$ (with $\sigma_{\pi N} \equiv \sigma_l^{(N)}$), from which the sigma term may be found. The precise value obtained this way has been under discussion for many years. However within the limits of our lattice calculation, this will not concern us here and for orientation we shall just quote a range of results from the earlier analyses of [3,4] of 45(8) MeV while a later dispersion analysis [5] suggested a much higher value 64(7) MeV. An estimation using heavy baryon chiral perturbation theory gave 45 MeV, [6]. A more recent estimate gave 59(17) MeV [7]. Even less is known about the nucleon strange sigma term. Equation (1) is usually written (in particular for the nucleon) as

$$\begin{aligned}\sigma_l^{(N)} &= \frac{m_l^R \langle N|(\bar{u}u + \bar{d}d - 2\bar{s}s)^R|N\rangle}{1 - y^{(N)R}}, \\ y^{(N)R} &= \frac{2\langle N|(\bar{s}s)^R|N\rangle}{\langle N|(\bar{u}u + \bar{d}d)^R|N\rangle},\end{aligned} \tag{2}$$

(i.e. we consider $\sigma_l^{(N)}$ and $y^{(N)R}$ rather than $\sigma_l^{(N)}$ and $\sigma_s^{(N)}$). The simplest calculation, e.g. [1] (which we will discuss in more detail later) uses first order in $SU(3)$ flavor symmetry (octet) breaking to give

$$\sigma_l^{(N)} = \frac{m_l^R}{m_s^R - m_l^R} \frac{M_\Xi + M_\Sigma - 2M_N}{1 - y^{(N)R}} \sim \frac{26}{1 - y^{(N)R}} \text{ MeV}, \tag{3}$$

and

$$\sigma_s^{(N)} = \frac{m_s^R}{m_l^R} \frac{1}{2} y^{(N)R} \sigma_l^{(N)} \sim 325 \frac{y^{(N)R}}{1 - y^{(N)R}} \text{ MeV}, \tag{4}$$

[1]Or more accurately as the matrix element of the double commutator of the Hamiltonian with two axial charges. However this is equivalent to the definition given in Eq. (1), see for example [1].

where m_s^R/m_l^R is the ratio of the strange to light quark masses, which using the leading order partially conserved axial current (PCAC) formula for this ratio gives

$$m_s^R/m_l^R = (2M_K^2 - M_\pi^2)/M_\pi^2 \sim 25. \tag{5}$$

The Zweig rule, $\langle N|(\bar{s}s)^R|N\rangle \sim 0$ would then give

$$\sigma_l^{(N)} \sim 26 \text{ MeV}, \qquad \sigma_s^{(N)} \sim 0 \text{ MeV}, \tag{6}$$

while any nonzero strangeness content, $y^{(N)R} > 0$ would increase this value of $\sigma_l^{(N)}$, $\sigma_s^{(N)}$ (and indeed, due to the large coefficient, $\sigma_s^{(N)}$ quite rapidly).

Determination of the strange sigma term (and in particular $y^{(N)R}$) is important in constraining the cross section for the detection of dark matter. Weakly interacting massive particles (WIMPs) would be scattered off nuclei by the exchange of scalar particles, such as the standard model Higgs particle, which will interact more strongly with heavier quark flavors. This coupling can be parameterized in terms of the fractional contribution of a quark flavor q to the nucleon's mass M_N, $f_{T_q} = m_q^R\langle N|(\bar{q}q)^R|N\rangle/M_N$. While the contributions of the charm and heavier flavors approach a constant that is proportional to the gluonic contribution f_{T_g}, there is a strong dependence of the cross section on the value of f_{T_s}, see e.g. [8,9] and references therein.

Computing the sigma terms from lattice QCD has a long history from initial quenched simulations to 2 flavor and more recently $2+1$ flavor simulations, e.g. [10–21], with a status report being given in [22]. In general more recent results tend to give a lower $\sigma_s^{(N)}$ term than earlier determinations.

In this article, we shall investigate this simple picture as described in Eqs. (3) and (5) and, in particular, test the linearity assumption of $SU(3)$ flavor symmetry breaking.

II. FLAVOR SYMMETRY EXPANSIONS

Lattice simulations start at some point in the (m_s^R, m_l^R) plane and then approach the physical point (m_s^{R*}, m_l^{R*}) along some path. (In the future we shall denote the physical point with a $*$.) As we shall be considering flavor symmetry breaking then we shall start here at a point on the flavor symmetric line $m_l^R = m_s^R$ and then consider the path keeping the average quark mass constant, $\bar{m} = \text{const.}$. The $SU(3)$ flavor group (and quark permutation symmetry) then restricts the quark mass polynomials that are allowed, [23], giving for the baryon octet

$$M_H = M_0(\bar{m}) + c_H\delta m_l + O(\delta m_l^2), \tag{7}$$

with

$$c_H = \begin{cases} 3A_1 & H = N \\ 3A_2 & H = \Lambda \\ -3A_2 & H = \Sigma \\ -3(A_1 - A_2) & H = \Xi \end{cases} \tag{8}$$

where

$$\delta m_l = m_l - \bar{m}, \qquad \bar{m} = \tfrac{1}{3}(2m_l + m_s) \tag{9}$$

and A_1 and A_2 are unknown coefficients. So to linear order in the quark mass, we only have two unknowns (rather than four). A similar situation also holds for the pseudoscalar and vector octets (one unknown) and baryon decuplet (also one unknown). These functions highly constrain the numerical fits. At $O(\delta m_l^2)$ only the baryon decuplet has a further constraint.

Permutation invariant functions of the masses X_S, (or "center of mass" of the multiplet) can be defined and have no linear dependence on the quark mass. For example for the baryon octet we have

$$X_N = \tfrac{1}{3}(M_N + M_\Sigma + M_\Xi) = M_0(\bar{m}) + O(\delta m_l^2). \tag{10}$$

(The corresponding result for the pseudoscalar octet is given later in Eq. (29).)

Furthermore expanding about a specific fixed point, $m_l = m_s = m_0$ on the flavor symmetric line and allowing $\bar{m}$ to vary, we then have

$$M_0(\bar{m}) = M_0(m_0) + M_0'(m_0)(\bar{m} - m_0) + O((\bar{m} - m_0)^2). \tag{11}$$

We will see that A_1, A_2 give all the nonsinglet hyperon sigma terms and $M'(m_0)$ the singlet terms.

As an example of the quark mass expansion from a point on the flavor symmetric line in Fig. 1 we plot the baryon octet M_H/X_N for $H = N, \Lambda, \Sigma, \Xi$ against M_π^2/X_π^2 together with a linear fit, Eq. (7) and implicitly Eq. (29) using $2+1$ $O(a)$ improved clover fermions at $\beta = 5.50$, [24] using two starting values for the quark mass on the flavor symmetric line, namely $\kappa_0 = 0.12090, 0.12092$.

All the points have been arranged in the simulation to have constant $\bar{m}$. We see that a linear fit provides a good description of the numerical data from the symmetric point (where $M_\pi \sim X_\pi^* = 410.9$ MeV) down to the physical pion mass.

In a little more detail, the bare quark masses are defined as

$$am_q = \frac{1}{2}\left(\frac{1}{\kappa_q} - \frac{1}{\kappa_{0;c}}\right), \quad \text{with} \quad q = l, s, 0 \tag{12}$$

(with the index $q = 0$ denoting the common quark along the flavor symmetric line) and where vanishing of the quark mass along the $SU(3)$ flavor symmetric line determines $\kappa_{0;c}$. Keeping $\bar{m} = \text{constant} \equiv m_0$ gives

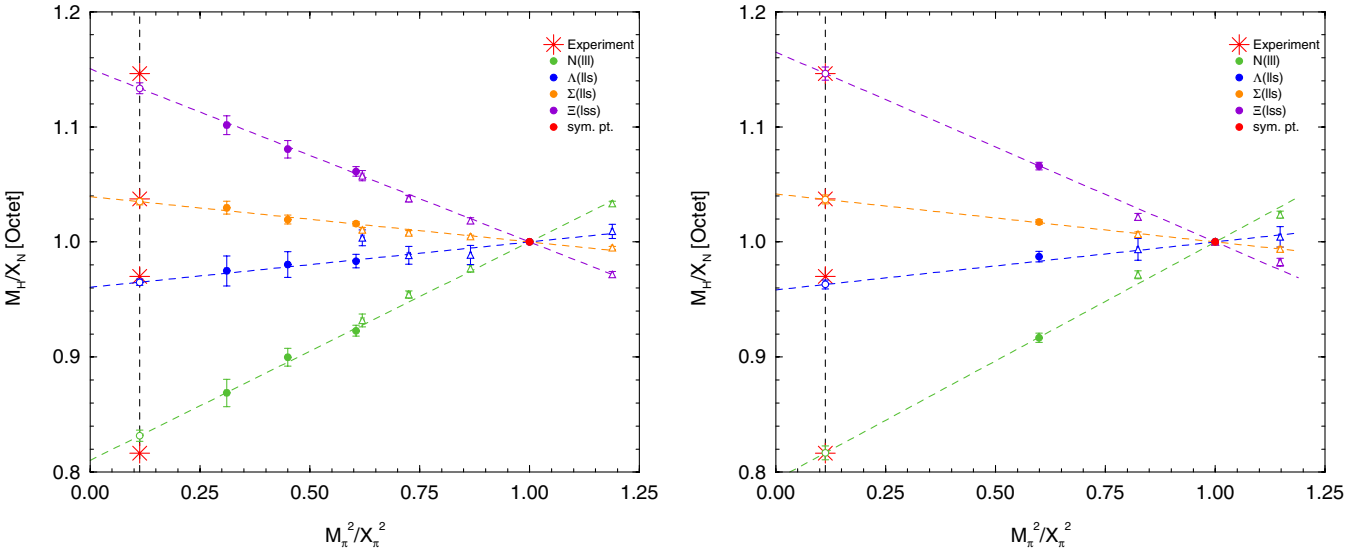

FIG. 1 (color online). M_H/X_N ($H = N, \Lambda, \Sigma, \Xi$) against M_π^2/X_π^2 for initial point ("sym. pt.") on the flavor symmetric line given by $\kappa_0 = 0.12090$ (left panel) and $\kappa_0 = 0.12092$ (right panel). The $32^3 \times 64$ lattices are filled circles, while the $24^3 \times 48$ lattices are open triangles. Also shown is the combined fit of Eq. (33) (dashed lines) to the $32^3 \times 64$ lattice data. The fit results are the open circles, while the experimental points are the stars. l and s denote the light and strange quark content of the hadron.

$$\kappa_s = \frac{1}{\frac{3}{\kappa_0} - \frac{2}{\kappa_l}}. \tag{13}$$

So once we decide on a κ_l this then determines κ_s. Note that $\kappa_{0;c}$ drops out of Eq. (13), so we do not need its explicit value. These initial κ_0 values chosen here, namely $\kappa_0 = 0.12090$ and 0.12092 are close to the path that leads to the physical point ($\kappa_0 = 0.12092$ being slightly closer). (This is discussed in more detail in [23], which also contains numerical tables and phenomenological values for the hadron masses. Results not included there are given in Appendix C.) This path is also illustrated later in Sec. IV C. Although finite size effects tend to cancel in ratios of quantities from the same multiplet, we nevertheless fit just to the results from the $32^3 \times 64$ lattices (filled circles) using the linear fit of Eq. (7). Finally note that we also have a similar flavor expansion for the pseudoscalar octet as for the baryon octet, as will be discussed in Sec. IV C.

III. (HYPERON) SCALAR MATRIX ELEMENTS

Scalar matrix elements can be determined from the gradient of the hadron mass (with respect to the quark mass) by using the Feynman-Hellman theorem which is true for both bare and renormalized quantities. So if we take the derivative with respect to the bare quark mass we get the bare $\bar{q}q$ matrix element,

$$\frac{\partial M_H}{\partial m_l} = \langle H|(\bar{u}u + \bar{d}d)|H\rangle, \quad \frac{\partial M_H}{\partial m_s} = \langle H|\bar{s}s|H\rangle, \tag{14}$$

while if we take the derivative with respect to the renormalized quark mass we get the renormalized matrix element. In the left panel of Fig. 2, we show the nucleon (diamonds) and the flavor symmetric nucleon (squares) against $1/\kappa_l$, $1/\kappa_0$ respectively [from Eq. (12) these are proportional to the bare quark mass]. From the Feynman-Hellmann theorem, the slope of the masses (squares) curve gives the total $\sum_{q=u,d,s}\langle N|\bar{q}q|N\rangle$, while the slope of the curve gives the valence contribution.[2] The difference between the two contributions gives the disconnected contribution. Because here all three quark masses are equal, the disconnected contribution for all three quarks will be the same. The two slopes thus give the estimates

$$\frac{\sum_q \langle N|\bar{q}q|N\rangle_{\text{con}}}{\sum_q \langle N|\bar{q}q|N\rangle} \sim \frac{4.0}{9.7} \sim 0.41, \tag{15a}$$

$$\frac{\langle N|\bar{s}s|N\rangle}{\sum_q \langle N|\bar{q}q|N\rangle} \sim \frac{1}{3}\left(\frac{9.7 - 4.0}{9.7}\right) \sim 0.19, \tag{15b}$$

for bare lattice quantities.

[2]Equation (7) can be extended to the "partially quenched" case [23], where the sea quark masses remain constrained by $\bar{m} = \text{const.}$ but the valence quark masses μ_l, μ_s are unconstrained. Defining $\delta\mu_q = \mu_q - \bar{m}$ then for the nucleon, the leading change is particularly simple, $c_N \delta m_l \to c_N \delta\mu_l$. For the other members of the octet, Λ, Σ, Ξ, both $\delta\mu_l$, $\delta\mu_s$ occur [23].

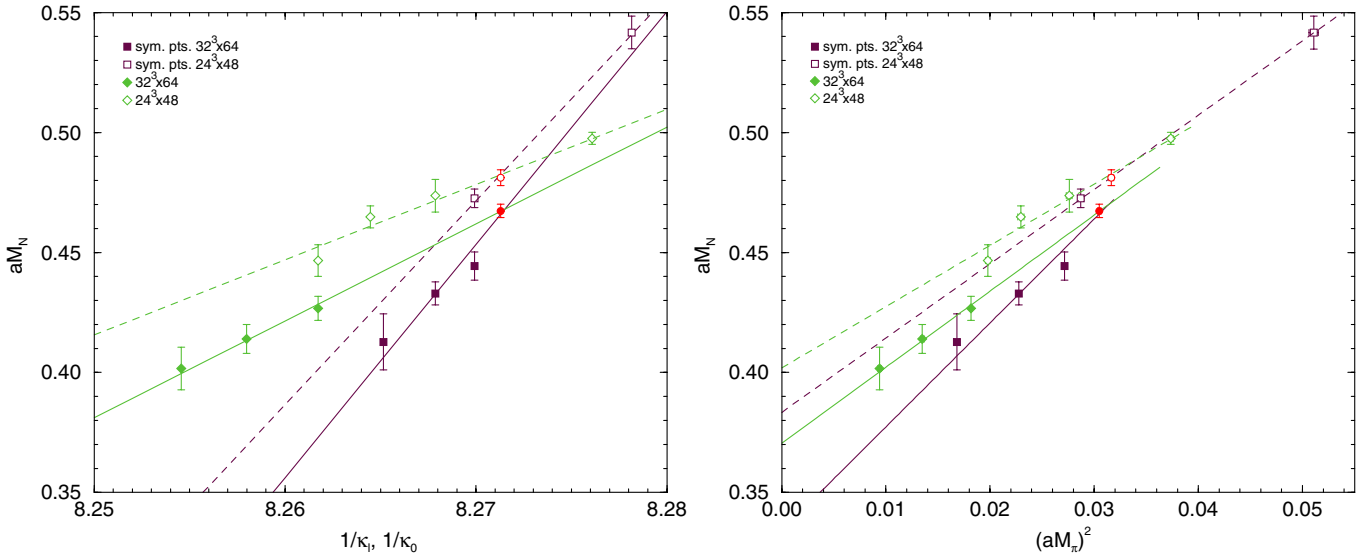

FIG. 2 (color online). The left panel shows the nucleon mass, aM_N, versus $1/\kappa_l$ (for the $\bar{m} = \text{const.}$ points, diamonds with $\kappa_0 = 0.12090$) and versus $1/\kappa_0$ (for the flavor symmetric points, "sym. pts.," squares). The common flavor symmetric points are denoted by circles. The $24^3 \times 48$ volume results are open circles together with a dashed line for the (linear) fit, while the $32^3 \times 64$ volume results are filled circles and lines. Similarly the right panel shows the nucleon mass aM_N, versus $(aM_\pi)^2$ (same notation as for the left panel).

To look at renormalized matrix elements, we need a plot against the renormalized mass, $(aM_\pi)^2$ [as in leading order PCAC, M_π^2 is proportional to the renormalized quark mass, Eq. (31)]. This is shown in the right panel of Fig. 2. The slopes are now much closer to each other. We now find the estimates

$$\frac{\sum_q \langle N|(\bar{q}q)^R|N\rangle_{\text{con}}}{\sum_q \langle N|(\bar{q}q)^R|N\rangle} \sim \frac{3.2}{4.3} \sim 0.74, \tag{16a}$$

$$\frac{\langle N|(\bar{s}s)^R|N\rangle}{\sum_q \langle N|(\bar{q}q)^R|N\rangle} \sim \frac{1}{3}\left(\frac{4.3-3.2}{4.3}\right) \sim 0.085, \tag{16b}$$

for renormalized lattice quantities, giving $y^{(N)R} \sim 2 \times 0.085/(1-0.085) \sim 0.19$. So although for bare matrix elements there is a significant strange quark content this is reduced in the renormalized matrix element.

We shall now try to make these considerations a little more quantitive.

IV. (HYPERON) σ EQUATIONS

A. Renormalization

For Wilson (clover) fermions under renormalization the singlet and nonsinglet pieces of the quark mass renormalize differently [25,26]. We have

$$m_q^R = Z^{NS}\left[m_q + \alpha_Z \frac{1}{3}(2m_l + m_s)\right], \qquad \alpha_Z = \frac{Z^S - Z^{NS}}{Z^{NS}}. \tag{17}$$

In the action the term $\sum_q m_q \bar{q}q = \sum_q m_q^R (\bar{q}q)^R$ i.e. a renormalization group invariant or RGI quantity. Upon writing this in a matrix form and inverting gives

$$(\bar{q}q)^R = \frac{1}{Z^{NS}}\left[\bar{q}q - \frac{\alpha_Z}{1+\alpha_Z}\frac{1}{3}(\bar{u}u + \bar{d}d + \bar{s}s)\right], \tag{18}$$

so for $\alpha_Z \neq 0$ then there is always mixing between bare operators.

As an example of where this manifests itself, the relation between the bare, $y^{(H)}$, and renormalized $y^{(H)R}$, cf. Equation (2), is then given by

$$y^{(H)R} = \frac{y^{(H)} - \frac{2}{3}\alpha_Z(1-y^{(H)})}{1 + \frac{1}{3}\alpha_Z(1-y^{(H)})}, \tag{19}$$

so we see that $y^{(H)R} \neq y^{(H)}$ for clover fermions. Additionally, since $\alpha_Z > 0$ and $y^{(H)} \gtrsim 0$ we find that $y^{(H)R} < y^{(H)}$, i.e. reduced.

Useful quark combinations are the octet and singlet combinations, namely

$$(\bar{u}u + \bar{d}d)^R - 2(\bar{s}s)^R = \frac{1}{Z^{NS}}[(\bar{u}u + \bar{d}d) - 2(\bar{s}s)],$$
$$(\bar{u}u + \bar{d}d)^R + (\bar{s}s)^R = \frac{1}{Z^{NS}(1+\alpha_Z)}[(\bar{u}u + \bar{d}d) + (\bar{s}s)]. \tag{20}$$

Furthermore, by using the Feynman-Hellman theorem [Eq. (14)] with the hadron flavor expansion [Eq. (7) together with Eq. (11)] gives

$$\langle H|(\bar{u}u + \bar{d}d)^R - 2(\bar{s}s)^R|H\rangle = \frac{1}{Z^{NS}} c_H, \tag{21}$$

$$\langle H|(\bar{u}u + \bar{d}d)^R + (\bar{s}s)^R|H\rangle = \frac{1}{Z^{NS}} \frac{M_0'}{1 + \alpha_Z}. \tag{22}$$

Equation (21), the equation for the matrix element of an octet operator, only involves c_H (the hadron mass expansion keeping the singlet quark mass constant), while Eq. (22), the matrix element of a singlet operator, only involves M_0' (occuring when changing the singlet quark mass). Equation (21) also leads to Eq. (3) as discussed in the introduction.[3]

Finally note that the quantities

$$\begin{aligned} &(m_s - m_l)\langle H|(\bar{u}u + \bar{d}d) - 2\bar{s}s|H\rangle, \\ &(2m_l + m_s)\langle H|(\bar{u}u + \bar{d}d) + \bar{s}s|H\rangle, \end{aligned} \tag{23}$$

are RGI and all Z factors cancel when they are renormalized. Linear combinations of these two quantities are also RGI, in particular, the combination used previously of $\sigma_l^{(H)} + \sigma_s^{(H)} = \sum_q m_q \langle H|\bar{q}q|H\rangle$. However, $\sigma_l^{(H)}$ and $\sigma_s^{(H)}$ considered separately are not RGI; see Eqs. (17) and (18). The renormalized quantities are mixtures of the two lattice quantities, and α_Z is needed to relate lattice values to continuum values. Refering back to Fig. 2 we see that the bare lattice strange sigma term is much larger that the renormalized strange sigma term, due to a cancellation between the two terms in Eq. (18).

B. σ equations

Multiplying the renormalized quark mass, Eq. (17), together with Eqs. (21) and (22) [or more generally with Eq. (18)] we can find RGI combinations (i.e. a form where the renormalization constant Z^{NS} cancels). In particular we find

$$\sigma_l^{(H)} - 2r\sigma_s^{(H)} = \frac{3r}{1 + 2r}(1 + \alpha_Z) m_0 c_H, \tag{24}$$

$$\sigma_l^{(H)} + r\sigma_s^{(H)} = \frac{3r}{1 + 2r} m_0 M_0'(m_0), \tag{25}$$

where r is the ratio of quark masses

$$r \equiv \frac{m_l^R}{m_s^R}. \tag{26}$$

Thus we have to find the (fixed) coefficients $(1 + \alpha_Z)m_0 c_H$, $m_0 M_0'(m_0)$. We then determine the physical values of the sigma terms by extrapolating to the point where the quark mass ratio takes its physical value, i.e. $r = r^*$.

We observe that we have two simultaneous equations, which can be easily solved to give[4]

$$\begin{aligned} \sigma_l^{(H)} &= \frac{r}{1 + 2r}[(1 + \alpha_Z)m_0 c_H + 2m_0 M_0'(m_0)], \\ \sigma_s^{(H)} &= \frac{1}{1 + 2r}[-(1 + \alpha_Z)m_0 c_H + m_0 M_0'(m_0)]. \end{aligned} \tag{27}$$

We see that the smallness of $\sigma_l^{(H)}$ in comparison to $\sigma_s^{(H)}$ is certainly guaranteed by the presence of an additional r in its numerator. As $\sigma_s^{(H)} > 0$ we must also have $M_0'(m_0) > (1 + \alpha_Z)\max c_H$. These coefficients are also sufficient to determine $y^{(H)R}$, as can be seen either directly from Eq. (27) or from Eq. (22),

$$y^{(H)R} = 2\frac{-(1 + \alpha_Z)m_0 c_H + m_0 M_0'(m_0)}{(1 + \alpha_Z)m_0 c_H + 2m_0 M_0'(m_0)}. \tag{28}$$

Again, as seen in Sec. III, $y^{(H)R}$ only depends on gradients and not on the physical point.

It is now convenient to normalize the coefficients by X_N so we now need to find the coefficients $(1 + \alpha_Z)m_0 c_H / X_N(m_0)$ and $m_0 M_0'(m_0)/X_N(m_0)$.

C. Determination of the coefficients

The hint for determining the coefficients from our lattice data is given in Sec. III, where we consider gradients with respect to a renormalized or physical quantity—here taken as the pion mass. As in Eq. (7) we also have a similar expansion for the pseudoscalar octet,

$$M_\pi^2 = M_{0\pi}^2 + 2\alpha\delta m_l + O(\delta m_l^2) \tag{29}$$

(together with $M_K^2 = M_{0\pi}^2 - \alpha\delta m_l + O(\delta m_l^2)$, $M_{\eta_s}^2 = M_{0\pi}^2 - 4\alpha\delta m_l + O(\delta m_l^2)$). This gives a good representation of the data as can be seen from Fig. 12 of [23]. Analogously to Eq. (10) we can define a flavor singlet quantity

$$X_\pi^2 = \tfrac{1}{3}(2M_K^2 + M_\pi^2) = M_{0\pi}^2 + O(\delta m_l^2). \tag{30}$$

However, as well as Eq. (7), we have the additional constraint from PCAC

$$M_\pi^2 = 2B_0^R m_l^R \tag{31}$$

(together with $M_K^2 = B_0^R(m_l^R + m_s^R)$, $M_{\eta_s}^2 = 2B_0^R m_s^R$) which implies that

$$M_{0\pi}^2 = 2\alpha(1 + \alpha_Z)\bar{m}, \qquad \alpha = B_0^R Z^{NS}. \tag{32}$$

If we now consider an expansion in the (physical) pion mass then eliminating δm_l between Eq. (7) and (29) gives

[3]The RHS of Eq. (21) can be rewritten as $c_N/Z^{NS} = 3A_1/Z^{NS}$. Together with $M_\Xi + M_\Sigma - 2M_N = -9A_1\delta m_l = 3A_1(m_s^R - m_l^R)/Z^{NS}$ this gives Eq. (3). An alternative mass combination that also picks out the A_1 coefficient is $M_\Xi - M_\Lambda = -3A_1\delta m_l$.

[4]This leads to relations between the various sigma terms, which we list in Appendix A and where we also argue that they are always approximately true.

$$\frac{M_H}{X_N} = \left(1 - \left[(1+\alpha_Z) m_0 \frac{c_H}{X_N}\right]\right) + \left[(1+\alpha_Z) m_0 \frac{c_H}{X_N}\right] \frac{M_\pi^2}{X_\pi^2}, \tag{33}$$

from the point on the symmetric line $m_0 = \bar{m}$. Thus if we plot M_H/X_N versus M_π^2/X_π^2 (holding the singlet quark mass, $\bar{m}$ constant) then the gradient immediately yields $(1+\alpha_Z) m_0 c_H/X_N$. The only assumption is that the "fan" plot splittings remain linear in δm_l down to the physical point. In Fig. 1 we show this plot giving the results

$$(1+\alpha_Z) m_0 \frac{3A_1}{X_N} = 0.1899(55), \qquad 0.2066(68),$$
$$(1+\alpha_Z) m_0 \frac{3A_2}{X_N} = 0.03942(314), \qquad 0.04164(431), \tag{34}$$

for $\kappa_0 = 0.12090$, 0.12092, respectively.

Alternatively on the flavor symmetric line, $m_l = \bar{m}$ (i.e. $\delta m_l = 0$), so varying $\bar{m}$ from a point m_0 gives

$$M_\pi^2(\bar{m}) = M_{0\pi}^2(\bar{m}) = M_{0\pi}^2(m_0) + M_{0\pi}^{2\prime}(m_0)(\bar{m} - m_0) = 2\alpha(1+\alpha_Z)[m_0 + (\bar{m} - m_0)], \tag{35}$$

which gives $M_{0\pi}^{2\prime}(m_0) = 2\alpha(1+\alpha_Z)$. So now eliminating $(\bar{m} - m_0)$ between Eqs. (11) and (35) gives

$$\frac{X_N(\bar{m})}{X_N(m_0)} = \left(1 - \left[\frac{m_0 M_0'(m_0)}{X_N(m_0)}\right]\right) + \left[\frac{m_0 M_0'(m_0)}{X_N(m_0)}\right] \frac{X_\pi^2(\bar{m})}{X_\pi^2(m_0)}. \tag{36}$$

Again in a plot of $X_N(\bar{m})/X_N(m_0)$ versus $X_\pi^2(\bar{m})/X_\pi^2(m_0)$ the gradient immediately gives the required ratio $m_0 M_0'(m_0)/X_N(m_0)$. We have also replaced M_N by X_N

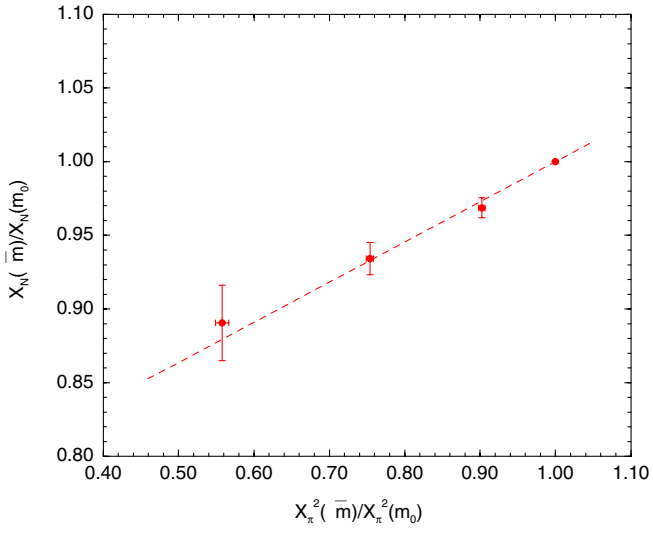

FIG. 3 (color online). $X_N(\bar{m})/X_N(m_0)$ versus $X_\pi^2(\bar{m})/X_\pi^2(m_0)$ along the flavor symmetric line, together with the linear fit from Eq. (36).

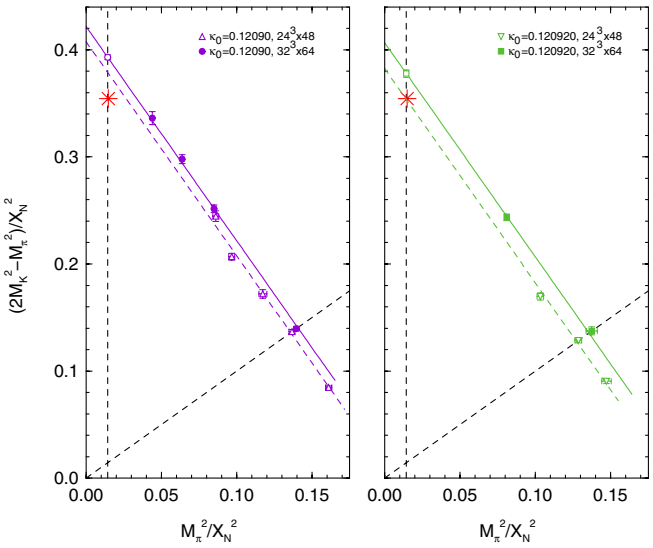

FIG. 4 (color online). $(2M_K^2 - M_\pi^2)/X_N^2$ versus M_π^2/X_N^2 for $\kappa_0 = 0.12090$ (left panel) and $\kappa_0 = 0.12092$ (right panel). The $32^3 \times 64$ volume results are given by the filled symbols, while the $24^3 \times 48$ volume results are shown using empty triangles. The fit is given in Eq. (38). Experimental points are denoted by stars.

and M_π^2 by X_π^2 (which allows us to use all the $32^3 \times 64$ data available for a particular $\bar{m}$). In Fig. 3 we plot $X_N(\bar{m})/X_N(m_0)$ versus $X_\pi^2(\bar{m})/X_\pi^2(m_0)$. From Eq. (36) this gives

$$\frac{m_0 M_0'(m_0)}{X_N(m_0)} = 0.273(32). \tag{37}$$

Finally the quark mass ratio, r, must be estimated. In Fig. 4 we plot $(2M_K^2 - M_\pi^2)/X_N^2$ versus M_π^2/X_N^2. From Eq. (29) we have

$$\frac{2M_K^2 - M_\pi^2}{X_N^2} = 3\frac{M_{0\pi}^2}{X_N^2} - 2\frac{M_\pi^2}{X_N^2}. \tag{38}$$

As in Sec. II, we see that for constant $\bar{m}$ the data points lie on a straight line (i.e. there is an absence of significant nonlinearity). Furthermore the gradient is fixed at -2. (Indeed leaving the gradient as a fit parameter for the $\kappa_0 = 0.12090$ confirms that this gradient is very close to -2.) Together with PCAC, Eq. (31) gives the x-axis as proportional to m_l^R while the y-axis is proportional to m_s^R and thus the ratio gives r. Taking our physical scale to be defined from $M_\pi^2/X_N^2|^*$ (i.e. from the x-axes of Fig. 4) gives

$$\frac{1}{r^*} = \frac{m_s^R}{m_l^R}\bigg|^* = \begin{cases} 27.28(16) & \kappa_0 = 0.12090 \\ 26.23(24) & \kappa_0 = 0.12092 \end{cases}. \tag{39}$$

D. Curvature effects

What can we say about corrections to the linear terms? The simple linear fit describes the data well, from the

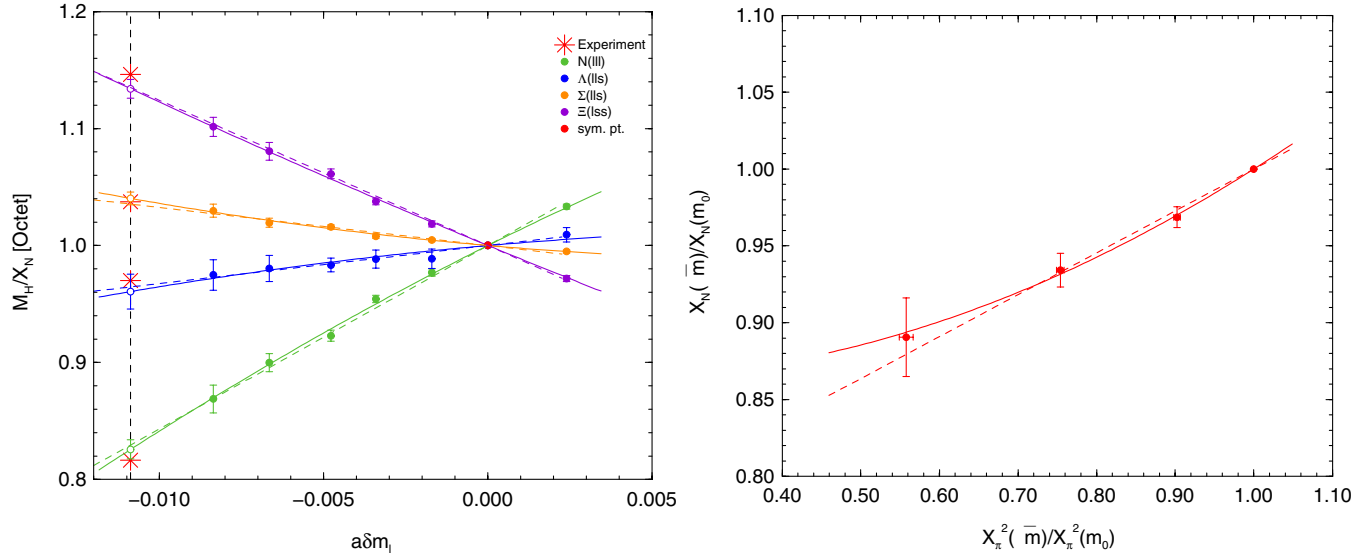

FIG. 5 (color online). Left panel: M_H/X_N for $H = N, \Lambda, \Sigma, \Xi$ against $a\delta m_l$ for initial point on the flavor symmetric line given by $\kappa_0 = 0.12090$ together with the previous linear fit (dashed lines) and quadratic fit (solid lines). Other notation as in Fig. 1. Right panel: $X_N(\bar{m})/X_N(m_0)$ versus $X_\pi^2(\bar{m})/X_\pi^2(m_0)$ along the flavor symmetric line, together with a linear fit from Eq. (36) (dashed line) and a quadratic fit (solid line).

symmetric point to our lightest pion mass, both along the $\bar{m} = \text{const.}$ line and the flavor symmetric line. To see the qualitatively of the possible influence of curvature we now compare linear fits with quadratic fits. These will be used to estimate possible systematic effects. We briefly discuss these effects here.

In Fig. 5 we compare the results of a quadratic fit and a linear fit, both for the baryon mass fan plot and for $X_N(\bar{m})/X_N(m_0)$. In the left panel of the figure, we consider the baryon mass fan plot. The quadratic fit here uses all the data, [23], on both lattice sizes (in cases where results for two lattice sizes are available, we used the larger lattice size only). The curvature terms here are small and statistically compatible with zero.

The right panel of the figure shows a quadratic fit to the results along the symmetric line. The curvature here is dominated by the large error of the lightest point (which has a low statistic). Thus we shall regard this fit as only giving an estimation of the possible systematic error.

The results in the next section include systematic error estimates from both these curvature sources combined in quadrature. In Appendix B we give some more details.

V. RESULTS

We can now numerically determine $y^{(H)R}$ and $\sigma_l^{(H)}$, $\sigma_s^{(H)}$.

We start with $y^{(H)R}$. From Eq. (28), together with Eqs. (34), (37), and (8) gives the results in Table I. The first error is the linear fit error [in this case dominated by the error in Eq. (37)], while the second error indicates possible effects from higher order terms, as discussed in Sec. IV D. We see that there is an order of magnitude increase in the fraction of $\langle H|(\bar{s}s)^R|H\rangle$ compared to $\langle H|(\bar{u}u + \bar{d}d)^R|H\rangle$ as we increase the strangeness content of the baryon from the nucleon (no valence strange quarks) to the Ξ (two valence strange quarks).

Turning to the sigma terms themselves, from Eq. (24) we can find an indication of the magnitude of $\sigma_l^{(N)}$ as approximately (with $X_N = 1.1501$ GeV),

TABLE I. Results for the baryon octet for $y^{(H)R*}$, $\sigma_l^{(H)*}$, $\sigma_s^{(H)*}$ with $H = N, \Lambda, \Sigma, \Xi$ for $\kappa_0 = 0.12090, 0.12092$.

	N	Λ	Σ	Ξ
$\kappa_0 = 0.12090$				
$y^{(H)R*}$	0.22(9)(15)	0.80(14)(28)	1.23(20)(41)	2.14(38)(64)
$\sigma_l^{(H)*}$ [MeV]	29(3)(4)	23(3)(4)	20(3)(4)	16(3)(5)
$\sigma_s^{(H)*}$ [MeV]	89(34)(59)	250(34)(68)	334(34)(68)	453(34)(58)
$\kappa_0 = 0.12092$				
$y^{(H)R*}$	0.18(9)(15)	0.79(14)(28)	1.25(20)(42)	2.30(42)(68)
$\sigma_l^{(H)*}$ [MeV]	31(3)(4)	24(3)(4)	21(3)(4)	16(3)(4)
$\sigma_s^{(H)*}$ [MeV]	71(34)(59)	247(34)(69)	336(34)(69)	468(35)(59)

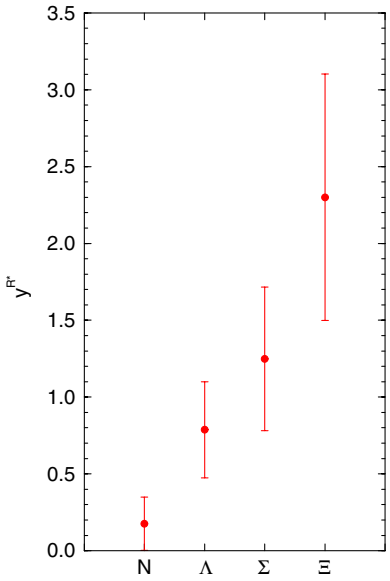

FIG. 6 (color online). $y^{(H)R*}$ for $H = N$, Λ, Σ, Ξ using the results from Table I for $\kappa_0 = 0.12092$.

$$\sigma_l^{(N)*} \sim [22 \sim 25] + \frac{\sigma_s^{(N)*}}{13}\ \text{MeV} > [22 \sim 25]\ \text{MeV} \tag{40}$$

(for $\kappa_0 = 0.12090$, 0.12092, respectively). The last inequality follows obviously as $\sigma_s^{(N)*} > 0$. Indeed this shows that a nonzero $\sigma_s^{(N)*} > 0$ can only add a few more MeV to this result.

The results for $\sigma_l^{(H)*}$ and $\sigma_s^{(H)*}$ are also given in Table I. (Again the first error is the statistical error, while the second systematic error is due to possible quadratic effects.) While the data for $\kappa_0 = 0.12090$ are more complete than for $\kappa_0 = 0.12092$ (cf. the plots in Fig. 1) and demonstrates linear behavior, as the path starting at $\kappa_0 = 0.12092$ is closer to the physical point (cf. Fig. 4), we shall use these values as our final values. These results are illustrated in Fig. 6 with $y^{(H)R*}$ for $H = N$, Λ, Σ, Ξ.

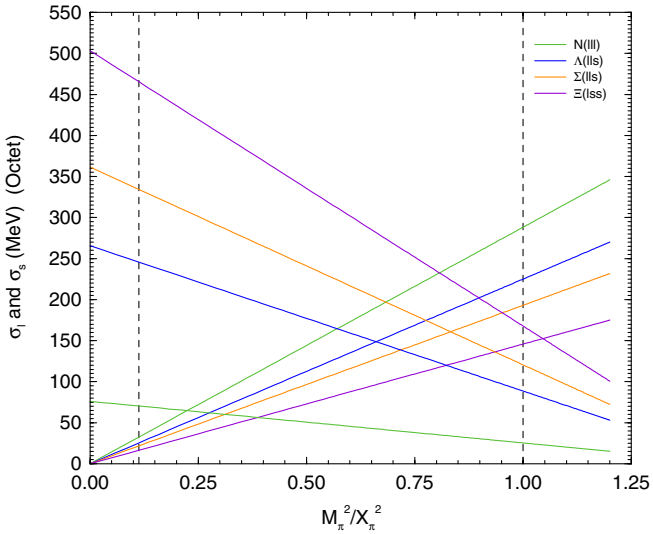

FIG. 7 (color online). $\sigma_l^{(H)}$ (decreasing from the symmetric point $x = 1$) and $\sigma_s^{(H)}$ (increasing) for $H = N$, Λ, Σ, Ξ for $\kappa_0 = 0.12092$. The physical and symmetric lines are denoted by vertical dashed lines. l and s denote the light and strange quark content of the hadron.

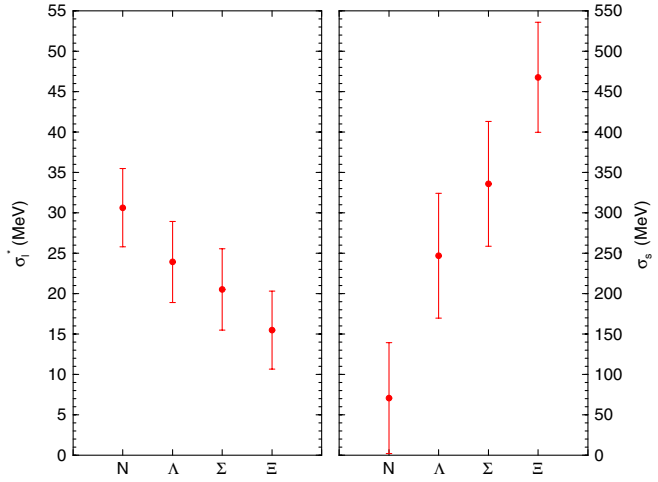

FIG. 8 (color online). $\sigma_l^{(H)*}$ and $\sigma_s^{(H)*}$ for $H = N$, Λ, Σ, Ξ at the physical point for $\kappa_0 = 0.12092$.

By varying r in Eq. (27),[5] we plot in Fig. 7 $\sigma_l^{(H)}$ and $\sigma_s^{(H)}$ for the baryon octet, $H = N$, Λ, Σ and Ξ from the symmetric point (vertical dashed line at $x = 1$) to the physical point (left vertical dashed line). $\sigma_l^{(H)}$ is rapidly decreasing while $\sigma_s^{(H)}$ is increasing as we decrease the quark mass. Also, as expected $\sigma_l^{(H)}$ is largest for the nucleon, N, while $\sigma_s^{(N)}$ is the smallest. Finally in Fig. 8 we plot $\sigma_l^{(H)*}$, $\sigma_s^{(H)*}$ against $H = N$, Λ, Σ and Ξ, again using Table I.

VI. CONCLUSIONS

Keeping the average quark mass constant gives very linear "fan" plots from the flavor symmetric point down to the physical point. This implies that an expansion in the quark mass from the flavor symmetric point will give information about the physical point. In this article we have applied this to estimating the sigma terms (both light and strange) of the nucleon octet. There has been no use of a chiral perturbation expansion (indeed this is an opposite expansion to the one used here, expanding about zero quark mass).

Our results are given in Sec. V and we quote from there a value for the nucleon sigma terms of

[5]Using, for example, the results from the left panel of Fig. 4, r may be rewritten as

$$r = \frac{M_\pi^2/X_\pi^2}{3 - 2(M_\pi^2/X_\pi^2)}.$$

$$\sigma_l^{(N)*} = 31(3)(4)\ \text{MeV}, \qquad \sigma_s^{(N)*} = 71(34)(59)\ \text{MeV}. \tag{41}$$

(The first error is the fit error while the second error indicates possible effects from higher order terms in the flavor expansion.) Note that expansions about the $SU(3)$ flavor line require consistency between many QCD observables, here, for example, not only for the baryon octet under consideration, but also for the pseudoscalar octet, PCAC and the ratio of the light to strange quark mass.

Of course there are several more avenues to investigate. Numerically an increase in statistics for the masses along the flavor symmetric line would reduce the dominant error (both statistical and systematic) and so directly help in decreasing the present errors. Our approach here has been to emphasize linearity at the expense (presently) of reaching exactly the physical point. This can be addressed by interpolating between a small set of constant $\bar{m}$ lines about the physical point. Additionally the use of partial quenching will also help to get closer to the physical pion mass. With more data, a systematic investigation of quadratic quark mass terms in the flavor expansion should be considered, to reduce the systematic errors. Finally while the use of linear or quadratic terms along the line of constant $\bar{m}$ is unproblematic, so that it is unlikely that Eq. (40) will change by much, more subtle is the relation involving $X(\bar{m})$ (i.e. the gradient when changing $\bar{m}$.) For the example of clover fermions we have $\tilde{g}^2(\bar{m}) = (1 + b_g a\bar{m})g^2$ which clearly does not change if $\bar{m} =$ constant, but will slightly change when $\bar{m}$ does. However this is probably not a large effect (as b_g seems small). For a discussion of some aspects of this issue see [27,28].

ACKNOWLEDGMENTS

The numerical configuration generation was performed using the BQCD lattice QCD program, [31], on the IBM BlueGeneL at EPCC (Edinburgh, United Kingdom), the BlueGeneL and P at NIC (Jülich, Germany), the SGI ICE 8200 at HLRN (Berlin-Hannover, Germany) and the JSCC (Moscow, Russia). We thank all institutions. The BlueGene codes were optimized using Bagel [32]. The Chroma software library [33] was used in the data analysis. This work has been supported in part by the EU Grants No. 227431 (Hadron Physics2), No. 238353 (ITN STRONGnet) and by the DFG under contract SFB/TR 55 (Hadron Physics from Lattice QCD). J. M. Z. is supported by STFC Grant No. ST/F009658/1.

APPENDIX A: SOME RELATIONS BETWEEN THE σ TERMS

We discuss here some relations between the sigma terms within a multiplet (here taken to be the baryon octet) which are exact within the linear case discussed, but which we might expect to always be approximately true.

The singlet relation Eq. (22) or Eq. (25) is the same for every hadron. So in terms of sigma terms this becomes

$$\sigma_l^{(H)} + r\sigma_s^{(H)} \approx \sigma_l^{(H')} + r\sigma_s^{(H')}. \tag{A1}$$

At the flavor symmetric point it follows from group theory that a singlet operator has the same value for every member of a multiplet, so Eq. (A1) must hold. But this can change if we move away from the symmetric point. (We shall briefly discuss this at the end of this section.)

We can find another collection of near identities by summing over a singlet combination of hadrons—this can be either a singlet of S_3 or a singlet of $SU(3)$. If we do this, the expectation values of $\bar{u}u$, $\bar{d}d$ and $\bar{s}s$ will be exactly equal at the flavor symmetry point, and stay again nearly equal away from the symmetry point. By this argument we expect

$$\begin{aligned} \sigma_l^{(\Lambda)} + \sigma_l^{(\Sigma)} &\approx 2r(\sigma_s^{(\Lambda)} + \sigma_s^{(\Sigma)}), \\ \sigma_l^{(N)} + \sigma_l^{(\Sigma)} + \sigma_l^{(\Xi)} &\approx 2r(\sigma_s^{(N)} + \sigma_s^{(\Sigma)} + \sigma_s^{(\Xi)}). \end{aligned} \tag{A2}$$

(Again this relation, as with the other relations discussed here, is exactly true for the linear case.)

Other relations come from the Gell-Mann Okubo relation, [29,30], in which the 27-plet mass combination is very small,

$$2M_N - 3M_\Lambda - M_\Sigma + 2M_\Xi \approx 0, \tag{A3}$$

for all values of m_l, m_s. In our approach, its derivatives are also near zero. We therefore expect

$$\begin{aligned} 2\sigma_l^{(N)} - 3\sigma_l^{(\Lambda)} - \sigma_l^{(\Sigma)} + 2\sigma_l^{(\Xi)} &\approx 0, \\ 2\sigma_s^{(N)} - 3\sigma_s^{(\Lambda)} - \sigma_s^{(\Sigma)} + 2\sigma_s^{(\Xi)} &\approx 0. \end{aligned} \tag{A4}$$

We obtain an even stronger version of these relations by taking the singlet combination, proportional to $(\bar{u}u + \bar{d}d)^R + (\bar{s}s)^R$,

$$\begin{aligned} &2\sigma_l^{(N)} - 3\sigma_l^{(\Lambda)} - \sigma_l^{(\Sigma)} + 2\sigma_l^{(\Xi)} \\ &\quad + r(2\sigma_s^{(N)} - 3\sigma_s^{(\Lambda)} - \sigma_s^{(\Sigma)} + 2\sigma_s^{(\Xi)}) \approx 0. \end{aligned} \tag{A5}$$

There is also a relation between the sigma terms and the hadron masses, [2], in the constants A_1 and A_2 which occur in the mass splittings also occur in the leading order expressions for the sigma terms. So there will be connections between masses and sigma terms. One particularly simple relation is

$$M_H - \sigma_l^{(H)} - \sigma_s^{(H)} \approx M_{H'} - \sigma_l^{(H')} - \sigma_s^{(H')}. \tag{A6}$$

(i.e. the baryon mass difference is closely accounted for by the sigma terms). For the linear case this is again exact, with this equation being equal to $M_0(m_0) - m_0 M_0'(m_0)$ for all the octet baryons [upon using Eqs. (7) and (27)]. From Eq. (11) we see that this is just the common hadron mass in the chiral limit along the flavor symmetric line, when

$m_l = 0 = m_s$ or $\bar{m} = 0$. $\sigma_l^{(H)}$ and $\sigma_s^{(H)}$ can be thought of as that part of the hadron mass which is due to m_l and m_s, respectively. The remnant, $M_0(m_0) - m_0 M_0'(m_0)$, is the part of the hadron mass due to the quark and gluon kinetic energy, interaction energy, etc., [2], i.e. the part of the hadron mass which is not due to the coupling with the Higgs vacuum expectation value.

We can use the higher order mass equations in [23] to estimate how well the relations in this section hold. Most of the relations have violations proportional to the first power of the $SU(3)$ breaking parameter, δm_l. The corrections to Eqs. (A1) and (A2) and the first relation in Eq. (A4) are $O(m_l \delta m_l)$. The σ_s relation in Eq. (A4) has corrections $O(m_s \delta m_l)$. When we combine these two relations to form Eq. (A5), the leading violation terms cancel, and we have a relation with corrections $O(m_l \delta m_l^2)$. The corrections to the mass relation Eq. (A6) are $O(\bar{m} \delta m_l)$ and $O(\delta m_l^2)$.

APPENDIX B: HIGHER ORDER EFFECTS

In this appendix, we discuss a little more quantitatively the systematic errors induced by the inclusion of the quadratic terms in the fit formulas. We concentrate particularly on the nucleon sigma terms, $\sigma_l^{(N)}$ and $\sigma_s^{(N)}$.

1. Curvature in the "fan" plot

In Fig. 5 we compare the results of a quadratic fit and a linear fit, both for the baryon mass fan plot and on $\sigma_l^{(N)}$ and $\sigma_s^{(N)}$. The quadratic fit uses all the data, [23], on both lattice sizes (in cases where results for two lattice sizes are available, we used the larger lattice size only). Including curvature terms in Eq. (7), [23], we have $M_H = M_0 + c_H \delta m_l + b_H \delta m_l^2 + \ldots$. Tracing through the analysis, we find the effect on Eq. (27) is to replace

$$c_H \rightarrow c_H + 2 b_H \delta m_l. \tag{B1}$$

By comparing c_H from the linear fit with $c_H + 2 b_H \delta m_l^*$ from the quadratic fit, we can estimate the maximum possible change.

We use the data at $\kappa_0 = 0.12090$, because this is the case where we have the most data covering the largest range in quark mass splitting, δm_l. In this case we have data covering about 3/4 of the gap from the symmetric point to the physical point, so we have the most chance of seeing curvature effects if they are present.

For the fan plot (left panel of Fig. 5), the curvature terms are found to be small, and statistically compatible with zero curvature. In Fig. 9 we compare the nucleon sigma terms from the slopes of the two fits by using Eq. (27) together with Eq. (B1). Again we see that the curvature effect is very small in the case of $\sigma_l^{(N)}$, particularly at small m_l, and much larger for $\sigma_s^{(N)}$. Can we explain this difference?

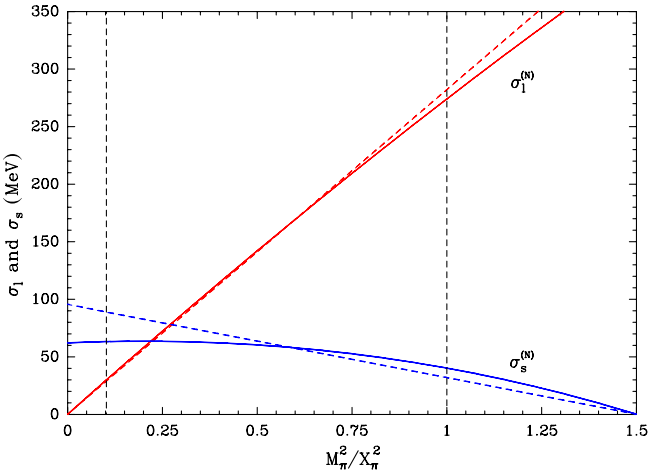

FIG. 9 (color online). $\sigma_l^{(N)}$ and $\sigma_s^{(N)}$ against M_π^2/X_π^2 using linear fits (dashed lines) and quadratic fits (solid lines) for $\kappa_0 = 0.12090$.

The slopes in the fan plot only effect the nonsinglet matrix element, the c_H term in Eq. (27). The curvature changes the slope of the nucleon line by about 10% at the physical point. The nonsinglet term in $\sigma_l^{(N)}$ is responsible for about 25% of the quantity, so a 10% change in slope translates to a 2.5% change in $\sigma_l^{(N)}$. Putting in the actual slope change, the final number we arrive at is a systematic uncertainty of about 1 MeV in $\sigma_l^{(N)}$ coming from curvature in the fan plot.

The situation for $\sigma_s^{(N)}$ is different, the singlet and nonsinglet terms appear with opposite signs, so $\sigma_s^{(N)}$ is given by the difference between two large quantities. Thus a 10% change in the nonsinglet matrix element is leveraged into a 25% change in $\sigma_s^{(N)}$. Repeating this procedure for the other hadrons gives similar nonsinglet uncertainties.

TABLE II. Additional result for the pseudoscalar octet mesons and octet baryons along the flavor symmetric line: aM_π, aM_N, for $(\beta, c_{sw}, \alpha) = (5.50, 2.65, 0.1)$.

κ_0	aM_π	aM_N
$32^3 \times 64$		
0.120920	0.1647(4)	0.4443(59)

TABLE III. Additional results for the pseudoscalar octet mesons: aM_π, aM_K and aM_{η_s} for $(\beta, c_{sw}, \alpha) = (5.50, 2.65, 0.1)$ where $\kappa_0 = 0.12092$.

(κ_l, κ_s)	aM_π	aM_K	aM_{η_s}
$24^3 \times 48$			
(0.120870, 0.121020)	0.1804(8)	0.1621(10)	0.1407(12)
(0.120980, 0.120800)	0.1545(9)	0.1775(8)	0.1976(7)

TABLE IV. Additional results for the octet baryons: aM_N, aM_Λ, aM_Σ and aM_Ξ for $(\beta, c_{sw}, \alpha) = (5.50, 2.65, 0.1)$ where $\kappa_0 = 0.12092$.

(κ_l, κ_s)	aM_N	aM_Λ	aM_Σ	aM_Ξ
$24^3 \times 48$				
(0.120870, 0.121020)	0.4812(40)	0.4721(62)	0.4672(48)	0.4618(58)
(0.120980, 0.120800)	0.4668(61)	0.4773(62)	0.4838(47)	0.4909(41)

TABLE V. Additional ratio results for the octet baryons: M_N/X_N, M_Λ/X_N, M_Σ/X_N and M_Ξ/X_N for $(\beta, c_{sw}, \alpha) = (5.50, 2.65, 0.1)$ where $\kappa_0 = 0.12092$.

(κ_l, κ_s)	M_N/X_N	M_Λ/X_N	M_Σ/X_N	M_Ξ/X_N
$24^3 \times 48$				
(0.120870, 0.121020)	1.024(3)	1.004(9)	0.9939(17)	0.9824(34)
(0.120980, 0.120800)	0.9715(33)	0.9934(95)	1.007(2)	1.022(3)
$32^3 \times 64$				
(0.121050, 0.120661)	0.9167(40)	0.9872(46)	1.017(2)	1.066(3)

2. Curvature along the symmetric line

We also use a linear fit to describe the baryon masses along the symmetric line (the line with all three quark masses equal). What is the effect of using a quadratic fit to determine the slope along this line?

In the right panel of Fig. 5 we compare a quadratic and linear fit to the symmetric baryon masses. As before, the quadratic term is compatible with zero curvature. Indeed the quadratic term is probably too large and is likely due to having a short lever arm and low statistics at the lightest point rather than to be a real effect. (Also we would expect that chiral perturbation theory would predict a downward curve.)

Feeding these values into Eq. (27) gives an estimate of the possible effect of quadratic terms, due to curvature along the symmetric line, which we will include in our final error estimate. This curvature effect is the same for every hadron, giving an uncertainty ~4 MeV for σ_l and ~55 MeV for σ_s. However because the shift is universal, this does not effect splittings, so the systematic error in $\sigma_l^{(H)} - \sigma_l^{(H')}$ is still given by the ~1 MeV value of the previous subsection. For $y^{(H)R}$, using the first equation in Eq. (4) gives percentage changes in $y^{(N)R}$ of 60% and 30% for $y^{(\Lambda)R}$, $y^{(\Sigma)R}$ and $y^{(\Xi)R}$.

APPENDIX C: HADRON MASSES

We collect here in Tables II, III, IV, and V numerical values for the meson pseudoscalar octet and baryon octet, not given in [23]. (All the data sets used here are over ~2000 configurations for the $24^3 \times 48$ volumes and ~1500–2000 configurations for the $32^3 \times 64$ volumes except for $\kappa_0 = 0.12099$ which has ~500 configurations.) Errors are from a bootstrap analysis.

[1] T.-P. Cheng and L.-F. Li, *Gauge Theory of Elementary Particles* (Oxford University, New York, 1988); *Computing Particle Properties*, edited by C. B. Lang and H. Gausterer (Springer-Verlag, Berlin, 1998).
[2] X. Ji, Phys. Rev. Lett. **74**, 1071 (1995).
[3] R. Koch, Z. Phys. C **15**, 161 (1982).
[4] J. Gasser, H. Leutwyler, and M. E. Sainio, Phys. Lett. B **253**, 252 (1991); **253**, 260 (1991).
[5] M. M. Pavan, I. I. Strakovsky, R. L. Workman, and R. A. Arndt, PiN Newslett. **16**, 110 (2002).
[6] B. Borasoy and U.-G. Meissner, Ann. Phys. (N.Y.) **254**, 192 (1997).
[7] J. Martin-Camalich, L. S. Geng, and M. J. Vicente Vacas, Phys. Rev. D **82**, 074504 (2010).
[8] J. Ellis, K. A. Olive, and P. Sandick, New J. Phys. **11**, 105015 (2009).
[9] J. Giedt, A. W. Thomas, and R. D. Young, Phys. Rev. Lett. **103**, 201802 (2009).
[10] S. Güsken, K. Schilling, R. Sommer, K. H. Mütter, and A. Patel, Phys. Lett. B **212**, 216 (1988).
[11] R. Altmeyer, M. Göckeler, R. Horsley, E. Laermann, and G. Schierholz (MTc Collaboration), Nucl. Phys. B, Proc. Suppl. **34**, 376 (1994); *Kyffhaeuser Workshop* (Leipzig, Germany, 1993).
[12] M. Fukugita, Y. Kuramashi, M. Okawa, and A. Ukawa, Phys. Rev. D **51**, 5319 (1995).
[13] S. J. Dong, J. F. Lagaë, and K. F. Liu, Phys. Rev. D **54**, 5496 (1996).

[14] S. Güsken, P. Ueberholz, J. Viehoff, N. Eicker, P. Lacock, T. Lippert, K. Schilling, A. Spitz, and T. Struckmann (SESAM Collaboration), Phys. Rev. D **59**, 054504 (1999).
[15] A. Walker-Loud, H.-W. Lin, K. Orginos, D. G. Richards, R. G. Edwards, M. Engelhardt, G. T. Flemming, Ph. Hägler, B. Musch, M. F. Lin, H. B. Meyer, J. W. Negele, A. V. Pochinsky, M. Procura, S. Syritsyn, C. J. Morningstar, D. B. Renner, and W. Schroers, Phys. Rev. D **79**, 054502 (2009).
[16] H. Ohki, H. Fukaya, S. Hashimoto, T. Kaneko, H. Matsufuru, J. Noaki, T. Onogi, E. Shintani, and N. Yamada (JLQCD Collaboration), Phys. Rev. D **78**, 054502 (2008).
[17] R. D. Young and A. W. Thomas, Phys. Rev. D **81**, 014503 (2010).
[18] K.-I. Ishikawa, N. Ishizuka, T. Izubuchi, D. Kadoh, K. Kanaya, Y. Kuramashi, Y. Namekawa, M. Okawa, Y. Taniguchi, A. Ukawa, N. Ukita, and T. Yoshié (PACS-CS Collaboration), Phys. Rev. D **80**, 054502 (2009).
[19] D. Toussaint and W. Freeman (MILC Collaboration), Phys. Rev. Lett. **103**, 122002 (2009).
[20] K. Takeda, S. Aoki, S. Hashimoto, T. Kaneko, J. Noaki, and T. Onogi (JLQCD Collaboration), Phys. Rev. D **83**, 114506 (2011).
[21] S. Dürr, Z. Fodor, T. Hemmert, C. Hoelbling, J. Frison, S. D. Katz, S. Krieg, T. Kurth, L. Lellouch, T. Lippert, A. Portelli, A. Ramos, A. Schäfer, and K. K. Szabó, Phys. Rev. D **85**, 014509 (2012).
[22] R. D. Young and A. W. Thomas, Nucl. Phys. **A844**, 266C (2010).
[23] W. Bietenholz, V. Bornyakov, M. Göckeler, R. Horsley, W. G. Lockhart, Y. Nakamura, H. Perlt, D. Pleiter, P. E. L. Rakow, G. Schierholz, A. Schiller, T. Streuer, H. Stüben, F. Winter, and J. M. Zanotti (QCDSF-UKQCD Collaboration), Phys. Rev. D **84**, 054509 (2011).
[24] N. Cundy, M. Göckeler, R. Horsley, T. Kaltenbrunner, A. D. Kennedy, Y. Nakamura, H. Perlt, D. Pleiter, P. E. L. Rakow, A. Schäfer, G. Schierholz, A. Schiller, H. Stüben, and J. M. Zanotti (QCDSF-UKQCD Collaboration), Phys. Rev. D **79**, 094507 (2009).
[25] M. Göckeler, R. Horsley, A. C. Irving, D. Pleiter, P. E. L. Rakow, G. Schierholz, and H. Stüben (QCDSF-UKQCD Collaboration), Phys. Lett. B **639**, 307 (2006).
[26] P. E. L. Rakow, Nucl. Phys. B, Proc. Suppl. **140**, 34 (2005).
[27] C. Michael, C. McNeile, and D. Hepburn, Nucl. Phys. B, Proc. Suppl. **106–107**, 293 (2002).
[28] R. Babich, R. C. Brower, M. A. Clark, G. T. Fleming, J. C. Osborn, C. Rebbi, and D. Schaich, arXiv:1012.0562.
[29] M. Gell-Mann, Phys. Rev. **125**, 1067 (1962).
[30] S. Okubo, Prog. Theor. Phys. **27**, 949 (1962).
[31] Y. Nakamura and H. Stüben, Proc. Sci., Lattice2010 (2010) 040 [arXiv:1011.0199].
[32] P. A. Boyle, Comput. Phys. Commun. **180**, 2739 (2009).
[33] R. G. Edwards and B. Joó, Nucl. Phys. B, Proc. Suppl. **140**, 832 (2005).